ARTICLES

Journal of Semiconductors
(2020) 41, 032101
doi: 10.1088/1674-4926/41/3/032101

Epitaxial graphene gas sensors on SiC substrate with high sensitivity

Cui Yu[1], Qingbin Liu[1], Zezhao He[1], Xuedong Gao[1], Enxiu Wu[2], Jianchao Guo[1], Chuangjie Zhou[1], and Zhihong Feng[1, †]

[1]National Key Laboratory of ASIC, Hebei Semiconductor Research Institute, Shijiazhuang 050051, China

[2]College of Precision Instrument and Opto-electronics Engineering, Tianjin University, Tianjin 300072, China

Abstract: 2D material of graphene has inspired huge interest in fabricating of solid state gas sensors. In this work, epitaxial graphene, quasi-free-standing graphene, and CVD epitaxial graphene samples on SiC substrates are used to fabricate gas sensors. Defects are introduced into graphene using SF_6 plasma treatment to improve the performance of the gas sensors. The epitaxial graphene shows high sensitivity to NO_2 with response of 105.1% to 4 ppm NO_2 and detection limit of 1 ppb. The higher sensitivity of epitaxial graphene compared to quasi-free-standing graphene, and CVD epitaxial graphene was found to be related to the different doping types of the samples.

Citation: C Yu, Q B Liu, Z Z He, X D Gao, E X Wu, J C Guo, C J Zhou, and Z H Feng, Epitaxial graphene gas sensors on SiC substrate with high sensitivity[J]. *J. Semicond.*, 2020, 41(3), 032101. http://doi.org/10.1088/1674-4926/41/3/032101

1. Introduction

Graphene is attractive for fabricating of solid state gas sensors due to its unique physical and chemical properties. It possesses large surface area per unit volume and zero charge carriers rest mass, and shows strong interaction with gas molecules due to physical or chemical adsorption[1–4]. After exposure and adsorption of targeted gas molecules, the electrical conductivity of graphene changes because of a change in carrier concentration of graphene. The electrical conductivity of graphene increases with target chemical species act as donor, and decreases for that act as acceptor. This phenomenon can be measured easily by an electronic system.

Several graphene allotropes, such as exfoliated graphene flakes[1, 5, 6], CVD graphene[7, 8] chemically reduced graphene oxide[9, 10], and epitaxial graphene (EG)[11–14], have been successfully used as gas sensors for ammonia, nitrogen oxides, sulfur oxides, and so on. EG grown on single crystal SiC substrate typically shows promising electrical properties, such as good surface morphology. In particular, due to the semi-insulator property of the SiC substrate, graphene does not need transfer to another substrate for device fabrication. This can avoid the possible processing pollutants that influence the sensing performance, such as the polymethylmethacrylaat (PMMA) that is usually used in the transfer process. These make EG on SiC a promising platform for gas sensors and easy up-scaling. Lebedev *et al.* demonstrated that UHV-grown epitaxial graphene give high sensitivity (5 ppb) to NO_2[14]. Novikov *et al.* used epitaxial graphene grown in Ar ambient to fabricate graphene gas sensor and NO_2 concentration of 0.2 ppb can be easily detected[15]. Iezhokin *et al.* used EG and quasi-free-standing epitaxial graphene (QFSEG) samples for gas sensors. They found for NO_2 gas, the sensitivity of QFSEG shows a six-fold increase compared to EG[13]. Samples show sensitivity better than 1 ppb. These results of graphene on SiC gas sensors are comparable to the current state-of-the-art solid state sensors[16, 17]. The defect-engineer has been shown to be an important way to the sensitivity improvement of graphene gas sensors. Kumar *et al.* used Ar plasma treatment and graphene gas sensors showed improved response[18]. Chung *et al.* used UV-ozone treatment to introduce defects in graphene[19]. Lee *et al.* used reactive ion etching (RIE) to fabricate defective graphene and found that graphene gas sensors show ultrahigh sensitivity with 33% improvement and 614% improvement in NO_2 and NH_3 sensing, respectively[7].

In this work, EG, QFSEG, and CVD grown epitaxial graphene (CVD-EG) on SiC substrates are used to fabricate graphene gas sensors. Defects are introduced into graphene using SF_6 plasma treatment with a conventional inductively coupled plasma (ICP) system to improve the performance of the graphene gas sensors.

2. Experiments

A 4H-SiC (0001) single-crystal wafer with chemical-mechanical polishing was first cut into pieces of 10 × 10 mm^2. Before graphene growth, the samples were cleaned with a conventional cleaning process, and then etched in hydrogen at 1550 °C for 6 min to remove the surface scratches. A regularly stepped surface formed on the SiC surface. Five graphene samples, named A–E were prepared in this work, as shown in Table 1. Samples A and B are EG grown by SiC sublimation method under Ar atmosphere at 1650 °C. More details about the graphene growth can be found in Ref. [20]. They show n type doping with sheet resistance R_s of 770 Ω/square, carrier mobility μ of 800 cm^2/(V·s), and sheet density N_s of 1 × 10^{13} cm^{-2}. Samples C and D are QFSEG grown by SiC sublimation and H intercalation by annealing the monolayer EG in hydrogen at 900 °C[21]. They show p type with sheet resistance R_s of 110 Ω/square, carrier mobility μ of

Correspondence to: Z H Feng, ga917vv@163.com
Received 12 AUGUST 2019; Revised 10 DECEMBER 2019.

Table 1. Graphene samples used for gas sensors.

Sample name	Graphene material	Growth method	SF_6 plasma treatment	Carrier type	Layer number
A	EG	SiC sublimation	Without	n	1
B	EG	SiC sublimation	7 s	n	1
C	QFSEG	SiC sublimation + H intercalation	10 s	p	2
D	QFSEG	SiC sublimation + H intercalation	7 s	p	2
E	CVD-EG	CVD	Without	p	1

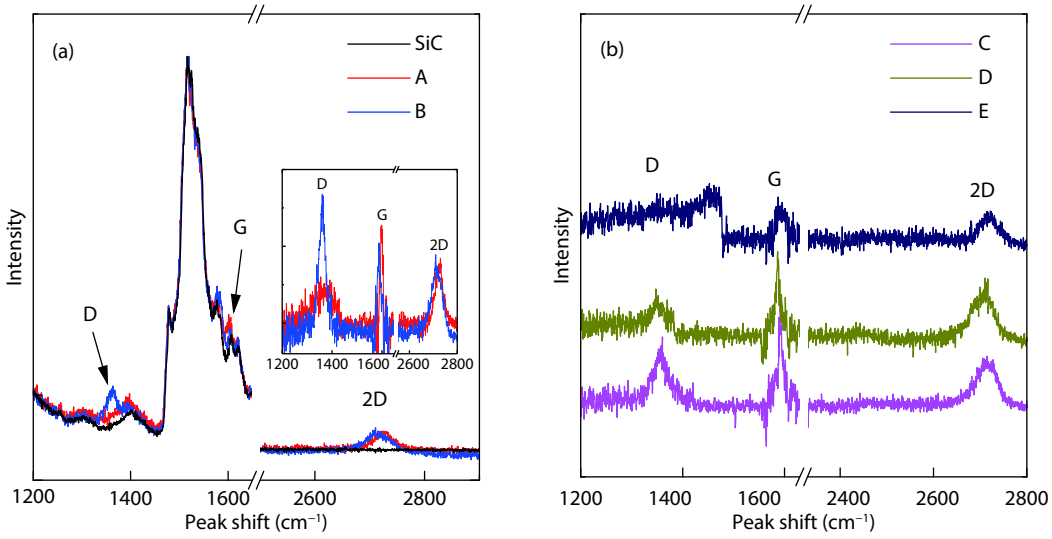

Fig. 1. (Color online) Raman spectra of (a) graphene samples A and B and the SiC substrate, and (b) graphene samples C, D, and E.

3200 $cm^2/(V{\cdot}s)$, and sheet density N_s of 1.8×10^{13} cm^{-2}. Sample E is CVD-EG. For the CVD growth of graphene, propane was the source gas, argon and hydrogen were carrier gases. The growth pressure was 900 mbar. The ratio of hydrogen to argon was 1 : 3. The sample shows p type with sheet resistance R_s of 770 Ω/square, carrier mobility μ of 500 $cm^2/(V{\cdot}s)$, and sheet density N_s of 1.6×10^{13} cm^{-2}. Samples B, C, and D were then treated by SF_6 plasma for 7, 10, and 7 s, respectively.

For EG sample grown on Si-face SiC substrate, a crucial feature is the existence of a buffer layer between epitaxial graphene and SiC surface. Unpaired electrons of the buffer layer lead to a series of partially occupied localized states, which makes epitaxial graphene n type doping[22]. For QFSEG sample, hydrogen atoms intercalated into the interface of graphene and SiC. The topmost Si atoms which for epitaxial graphene are covalently bound to this buffer layer, and are now saturated by hydrogen bonds. The buffer layer is turned into a quasi-free-standing graphene monolayer with its typical linear bands. Epitaxial monolayer graphene turns into a decoupled bilayer. The QFSEG samples show heavily p-type doping due to the polarization of the SiC substrate[23]. For CVD-EG sample, C_3H_8 and H_2 are used for the graphene growth. Due to the presence of H atoms, the CVD-EG in situ formed quasi-free-standing graphene in the growth process[24, 25].

Micro-Raman scattering measurements were performed at room temperature (RT) with a spectrometer at 514 nm. The carrier mobility, sheet density, and sheet resistance of all the graphene samples were measured at RT.

The resistance of the graphene gas sensors was measured by a four-probe method. The devices were measured in a chamber with atmospheric nitrogen environment at RT. Before measurement, the graphene samples were annealed in N_2 at 200 °C for 30 min to remove possible contamination of the graphene samples. The resistance of the graphene device was stable over several hours in a pure N_2 gas, which verify the inertness of graphene to nitrogen. The signal to noise ratio at base line is around 0.01. The test target gas was diluted by the N_2 carrier gas by a gas calibration system.

3. Results and discussion

The Raman spectra of the graphene samples A–E and the SiC substrate are shown in Fig. 1. Graphene contains two dominated Raman bands of G-band at ~1582 cm^{-1} and 2D band at ~2679 cm^{-1} (the second order of D-band)[26]. D peak around 1335 cm^{-1} is originated from the vacancy or disorder of carbon atoms, which can be used to reflect the number of defects in graphene. The Raman spectra of graphene on SiC substrate unavoidably contain apparent background peaks from the SiC substrate, as shown in Fig. 1. From Fig. 1, it can be found that samples B, C, and D shows obvious D peak, indicating that the SF_6 plasma treatment introduces some defects into the graphene lattice.

The performance of the five graphene gas sensors was measured and their corresponding sensitivity was calculated by[4]

$$\text{Response} = \frac{|R - R_0|}{R_0} \times 100, \tag{1}$$

where R_0 is the resistance prior of the device to exposure to the target gas and R is the resistance after exposure to the target gas molecules. Sensor responses for NO_2 and NH_3 gases, p- and n-type dopants to graphene, are represented in Fig. 2.

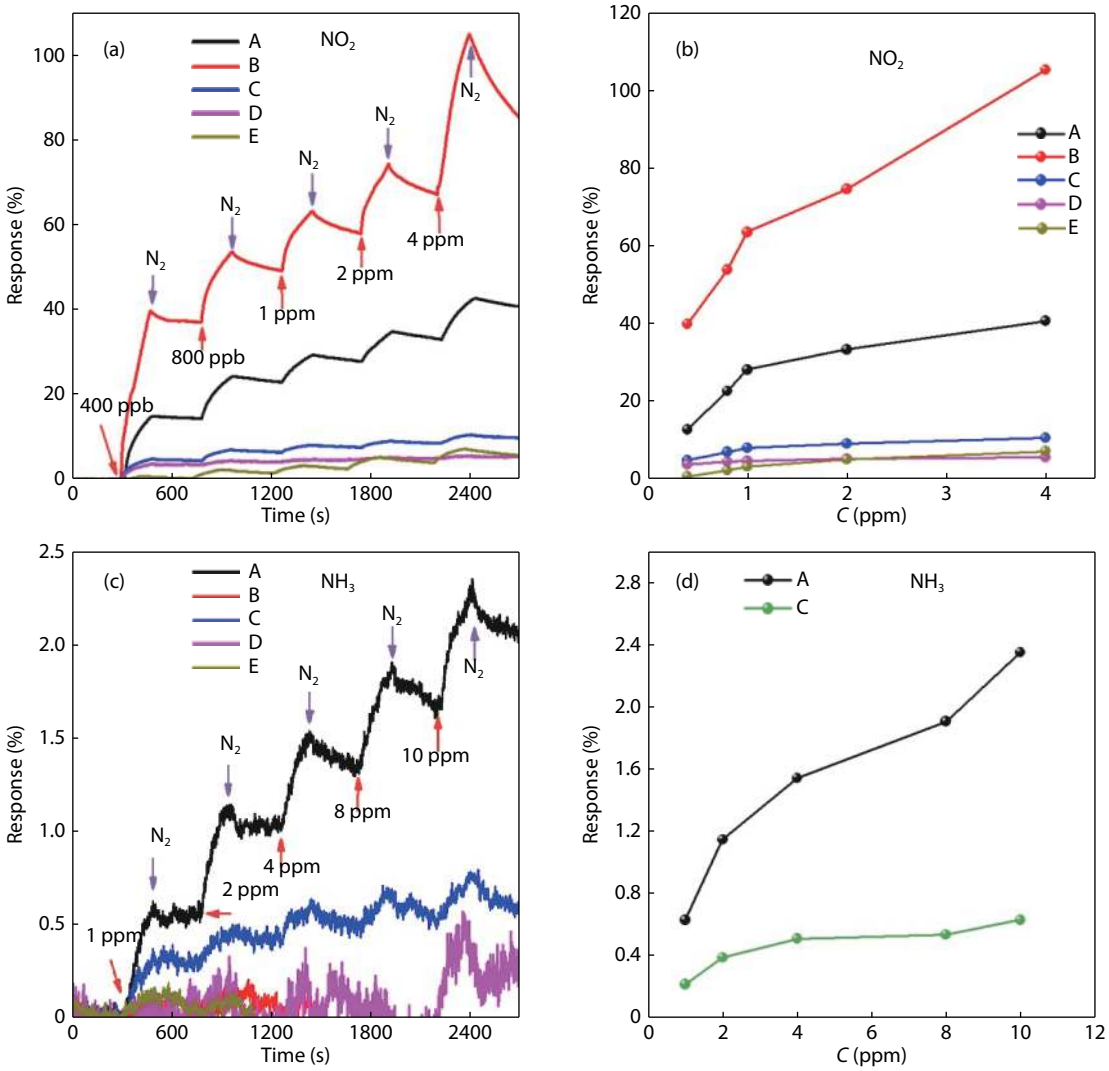

Fig. 2. (Color online) Sensor responses for (a, b) NO_2 and (c, d) NH_3.

Table 2. Sensitivity of the graphene gas sensors to NO_2 gas and their detection limit (DL).

Sample		Original resistance (Ω)	NO_2 concentration (ppm)					DL (ppb)
			0.4	0.8	1	2	4	
Sensitivity to NO_2 gas	A	335	14.0%	22.8%	28.2%	33.5%	40.8%	1
	B	396	40.0%	53.9%	63.5%	74.6%	105.1%	2
	C	292	5.0%	7.2%	8.3%	9.3%	10.7%	60
	D	315	4.0%	4.7%	5.0%	5.4%	5.8%	70
	E	296	0.9%	2.5%	3.4%	5.3%	7.4%	50

As shown in Fig. 2(a), all the graphene sensors show an obvious response to NO_2 gas. The sensitivity of the graphene samples shows nearly liner dependence with the NO_2 gas concentration at the lower concentration region (400 ppb to 1 ppm), as shown in Fig. 2(b) and Table 2. The response of EG (samples A and B) to NO_2 gas is much higher than the QFSEG (samples C and D) and CVD-EG (sample E). Compared with sample A, the defect-engineered sample B shows great improvement in the sensitivity to NO_2 gas. The detection limit was calculated by the sensor's signal processing performance by the following equation[27]

$$\mathrm{DL\ (ppm)} = 3\frac{\mathrm{rms}}{\mathrm{slope}}, \qquad (2)$$

where rms is the noise (signal to noise ratio at base line). The DL to NO_2 gas for samples A and B reached 1 and 2 ppb, respectively, indicating the high sensitivity of the EG samples to NO_2 gas. The DL to NO_2 gas for samples C, D and E were 60, 70, and 50 ppb, respectively.

QFSEG and CVD-EG samples (samples C, D, and E) show comparable response and DL to NO_2 gas. The EG samples (samples A and B) show much higher sensitivity to NO_2 gas than the QFSEG and CVD-EG samples. This may be due to the different doping types of the samples: samples A and B are n type doping; samples C, D, and E are p type doping; and, NO_2 gas is a well-known p-type dopant to graphene sample.

As illustrated in Fig. 3, a simple model was used to explain the different responses of graphene samples with differ-

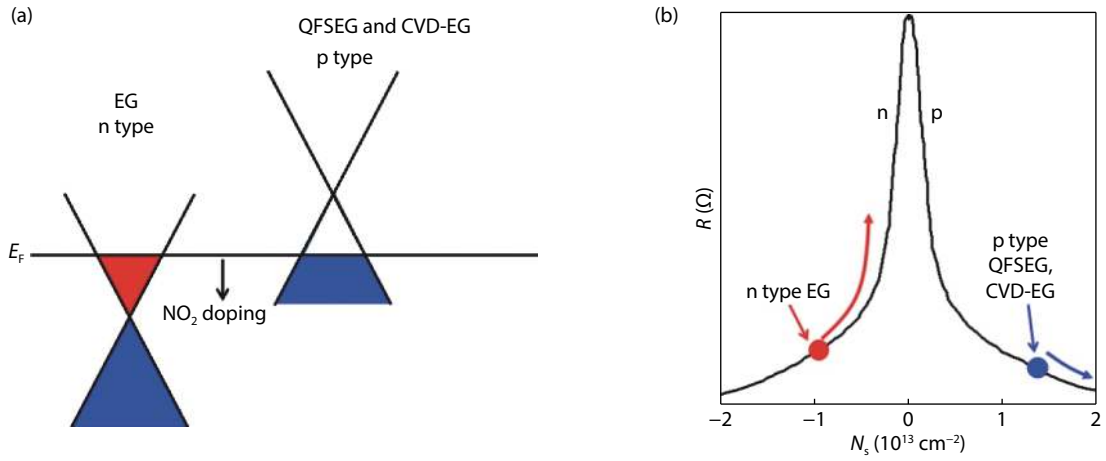

Fig. 3. (Color online) Schematic illustration of (a) the Fermi level shift and (b) resistance due to NO_2 doping for n-type EG and p-type QFSEG and CVD-EG.

ent doping types (samples A, C/D, and E). The Fermi energies of EG and QFSEG and CVD-EG are different (Fig. 3(a)). The EG samples are n type ($N_s = 1 \times 10^{13}$ cm^{-2}) due to the Fermi level pinning effect of the buffer layer[15]. After hydrogen intercalation in QFSEG, samples show heavily p-type doping ($N_s = 1.8 \times 10^{13}$ cm^{-2}) due to the polarization of the SiC substrate[23]. The CVD-EG is also heavily p-type doping ($N_s = 1.6 \times 10^{13}$ cm^{-2})[28]. The density states of graphene are proportional to the energy with linear relationship of $E \propto N_s$. Fig. 3(b) shows a schematic illustration of the relationship of resistance R and sheet density N_s of graphene[29]. For the n-type EG sample, the initial resistance point is on the left-hand side of the resistance peak, as shown in Fig. 3(b) by the red circle. Adsorbing of NO_2 molecules causes hole doping of the EG system, leading to shift of the resistance of the EG sample closer to the charge neutral point (CNP) point ($N_s = 0$). This will lead to a rapid increase in the resistance (sharp peak region). For the QFSEG and CVD-EG samples, the samples are p type with the initial point in the right side of the resistance peak. Adsorbing of NO_2 molecules also causes hole doping of the graphene, leading to the resistance shift away from the CNP point ($N_s = 0$). The change of resistance due to surface doping is smaller compared to the EG samples.

Compared with sample A, the defect-engineered sample B shows a great improvement in the sensitivity to NO_2 gas. The response of the graphene sensors to NH_3 is not the same with NO_2. Only samples A and C show responses to NH_3, as shown in Fig. 2(c). Other samples show no obvious response to NH_3. These results are consistent with the reported results and first-principles calculations[19, 30]. Theoretical studies have proven that compared to pristine graphene, adsorption of gas molecules is stronger on defective graphene than pristine graphene. Therefore, the introduction of defects into graphene remarkably improves the sensitivity of graphene gas sensor[30]. Zhang *et al.* found that gas molecules (NO_2, NH_3) and defective graphene show stronger interactions than with pristine graphene by DFT calculations. They found the adsorption energy of NO_2 gas molecule on defective graphene is –3.04 eV, and it is –0.48 eV for that of pristine graphene. Meanwhile, the charge transfer between NO_2 gas molecules and defective graphene (–0.38e) is also larger than pristine graphene (–0.19e)[30]. For NH_3 gas, the adsorption energy of NH_3 gas molecule on defective graphene (–0.24 eV) is higher than that on pristine graphene (–0.11 eV). However, the charge transfer between NH_3 gas molecules and defective graphene (–0.02e) is the same with that of pristine graphene (–0.02e). The calculated charge transfer is relatively small for NH_3 gas than that for NO_2 gas. The small charge transfer of graphene with NH_3 gas is in agreement with the weak response of the graphene gas sensor to NH_3 observed in the experiments.

4. Conclusions

Epitaxial graphene, quasi-free-standing graphene, and CVD epitaxial graphene samples on SiC substrates are used to fabricate gas sensors. The epitaxial graphene shows the highest sensitivity to NO_2 gas. This can be explained by the doping type and resistance-carrier density relation. The defect-engineered sample shows improved sensitivity to NO_2 with response of 105.1% to 4 ppm NO_2, which is consistent with the DFT calculations that both of the adsorption energies and charge transfer increased. The samples show weak response to NH_3 due to the small charge transfer. Our results show the application potential of epitaxial graphene on SiC to NO_2 gas detection.

Acknowledgements

This work was supported by the National Natural Science Foundation of China (61674131 and 61306006).

References

[1] Schedin F, Geim A K, Morozov S V, et al. Detection of individual gas molecules adsorbed on graphene. Nat Mater, 2007, 6, 652
[2] Geim A K, Novoselov K S. The rise of graphene. Nat Mater, 2007, 6, 183
[3] Novoselov K S, Falko V I, Colombo L, et al. A roadmap for graphene. Nature, 2012, 490, 192
[4] Varghese S S, Lonkar S, Singh K K, et al. Recent advances in graphene based gas sensors. Sens Actuators B, 2015, 218, 160
[5] Dan Y, Lu Y, Kybert N J, et al. Intrinsic response of graphene vapor sensors. Nano Lett, 2009, 9, 1472
[6] Rumyantsev S, Liu G, Shur M S, et al. Selective gas sensing with a single pristine graphene transistor. Nano Lett, 2012, 12, 2294
[7] Lee G, Yang G, Cho A, et al. Defect-engineered graphene chemic-

al sensors with ultrahigh sensitivity. Phys Chem Chem Phys, 2016, 18, 14198

[8] Singh A K, Uddin M A, Tolson J T, et al. Electrically tunable molecular doping of graphene. Appl Phys Lett, 2013, 102, 043101

[9] Toda K, Furue R, Hayami S. Recent progress in applications of graphene oxide for gas sensing: A review. Anal Chim Acta, 2015, 878, 43

[10] Li W, Geng X, Guo Y, et al. Reduced graphene oxide electrically contacted graphene sensor for highly sensitive nitric oxide detection. ACS Nano, 2011, 5, 6955

[11] Nomani M W K, Shishir R, Qazi M, et al. Highly sensitive and selective detection of NO_2 using epitaxial graphene on 6H-SiC. Sens Actuators B, 2010, 150, 301

[12] Pearce R, Iakimov T, Andersson M, et al. Epitaxially grown graphene based gas sensors for ultra sensitive NO_2 detection. Sens Actuators B, 2011, 155, 451

[13] Iezhokin I, Offermans P, Brongersma S H, et al. High sensitive quasi freestanding epitaxial graphene gas sensor on 6H-SiC. Appl Phys Lett, 2013, 103, 053514

[14] Lebedev A A, Lebedev S P, Novikov S N, et al. Supersensitive graphene-based gas sensor. Tech Phys, 2016, 61, 3, 453

[15] Novikov S, Lebedeva N, Satrapinski A. Graphene based sensor for environmental monitoring of NO_2. J Sen, 2015, 2015, 7

[16] Wetchakun K, Samerjai T, Tamaekong N, et al. Semiconducting metal oxides as sensors for environmentally hazardous gases. Sens Actuators B, 2011, 160, 580

[17] Zhang T, Mubeen S, Myung N V, et al. Recent progress in carbon nanotube-based gas sensors. Nanotechnology, 2008, 19, 332001

[18] Kumar B, Min K, Bashirzadeh M, et al. The role of external defects in chemical sensing of graphene field-effect transistors. Nano Lett, 2013, 13, 1962

[19] Chung M G, Kim D H, Lee H M, et al. Graphene-based composite materials for chemical sensor application. Sens Actuators B, 2012, 166/16, 172

[20] Yu C, Li J, Liu Q B, et al. Buffer layer induced band gap and surface low energy optical phonon scattering in epitaxial graphene on SiC (0001). Appl Phys Lett, 2013, 102, 013107

[21] Yu C, Liu Q B, Li J, et al. Preparation and electrical transport properties of quasi free standing bilayer graphene on SiC (0001) substrate by H intercalation. Appl Phys Lett, 2014, 105, 183105

[22] Pankratov O, Hensel S, Bockstedte M. Electron spectrum of epitaxial graphene monolayers. Phys Rev B, 2010, 82, 121416

[23] Ristein J, Mammadov S, Seyller T. Origin of doping in quasi-free-standing graphene on silicon carbide. Phys Rev Lett, 2012, 108, 246104

[24] Ciuk T, Strupinski W. Charge carrier concentration and offset voltage in quasi-free-standingmonolayer chemical vapor deposition graphene on SiC. Carbon, 2015, 93, 1042

[25] Ciuk T, Caban P, Strupinski W. Statistics of epitaxial graphene for Hall effect sensors. Carbon, 2016, 101, 431e438

[26] Ferrari A C. Raman spectroscopy of graphene and graphite: Disorder, electron–phonon coupling, doping and nonadiabatic effects. Solid State Commun, 2007, 143, 47

[27] Choi Y R, Yoon Y G, Choi K S, et al. Role of oxygen functional groups in graphene oxide for reversible room-temperature NO_2 sensing. Carbon, 2015, 91, 178

[28] Portail M, Michon A, Vezian S, et al. Growth mode and electric properties of graphene and graphitic phase grown by argon-propane assisted CVD on 3C-SiC/Si and 6H-SiC. J Cryst Growth, 2012, 349, 27

[29] Waldmann D, Jobst J, Speck F, et al. Bottom-gated epitaxial graphene. Nat Mater, 2011, 10, 357

[30] Zhang Y H, Chen Y B, Zhou K G, et al. Improving gas sensing properties of graphene by introducing dopants and defects: a first-principles study. Nanotechnology, 2009, 20, 185504